International Journal of Mechanical and Materials Engineering (IJMME), Vol.5 (2010), No.2, 208-213

PREDICTION OF HEAT FLOW THROUGH SAND MOULD AND ITS VERIFICATION ON THE STRUCTURE AND PROPERTY OF GRAY CAST IRON

S. K. Shaha, M. M. Haque and M. A. Maleque
Dept. of Manufacturing and Materials Engineering,
International Islamic University Malaysia, P.O. Box-10, 50728, Kuala Lumpur, Malaysia
Email: sugribshah_mme@yahoo.com

Received 12 November 2009, Accepted 26 June 2010

ABSTRACT

Heat flows through the mould in casting govern the cooling rate of the liquid which affects the structure and properties of the materials. By controlling the heat flow direction, it is possible to control the structures as well as properties of the materials. To predict the heat-flow through the sand mould, finite element (FE) model was developed using FEA software. In order to verify the FE model, the gray cast iron was melted at 1350 ^{0}C temperature and poured into the sand mould at 1300 ^{0}C. The predicted and experimentally verified results show that maximum heat-reserve at the junction of the mould and the minimum at the end of the mould which increases with time at the thick section (10 mm). As a consequence, the solidification rate is higher at the end of the mould wall whereas it is comparatively lower near the sprue of the mould. It also shows that the microstructure and hardness change due to different heat flow through the sand mould.

Keywords: Simulation; Sand mould; Casting; Microstructure.

1. INTRODUCTION

Solidification of materials is the most important phenomena to get desire structure which drive the properties of the materials. The whole solidification process consists of three different stages: nucleation, growth and impingement (Chao and Du, 1999). When the liquid metal temperature starts to decrease and goes below the melting point, the nucleation begins and crystal cluster formed which are continuously formed and remelt. However, when the temperature is low enough then the clusters are at stable condition and do not remelt any more. In the initial stage, this process occurs very slowly and when critical cooling temperature is reached, it grows very rapidly and the grain forms. After that, the radii increase until the grains touch each other in where still some liquid are present among or inside the grains. In the final stage, the liquid solidify and the radii cannot increase any more (Seetharamu et al., 2001). Casting is the most important process in manufacturing section and sand casting is the most convenient process in foundry. Most of the liquid metal can be poured into the sand mould without any size. Now-a-days, this sand casting getting popular for the production of many engineering products and components. The use of powerful software and programme to control the quality of the process materials and major interest in the present state of art which is reduced the wastage of materials and save the cost of the final product. Solidification rate of molten metal in the sand mould depends on the thermal conductivity of the mould material, casting design, the direction of heat-flow into the mould wall, etc. If the heat-flow through the mould is very quick, the solidification rate will be higher at that point and will affect the microstructure and properties of the materials. Heat-flow through the sand mould was studied by many researchers and their achievement and limitations discuss below.

Al-Asady et al. (2009) cited that the finite element analysis (FEA) has become a powerful tool for the numerical solution of a wide range of engineering problems. Seetharamu et al. (2001) studied the solidification phenomena in sand mould for thermal stress using FEA and they discussed about the effect of solidification on stress formation in casting. Pequet et al. (2002) studied the defects formation during solidification of Al alloy using ABAQUS and showed that most of the defects formed where the metal solidified last. Sulaiman and Hamouda (2004) investigated the thermal history of the sand casting process for mould filling time using FORTRAN. They have shown that the lastly solidifying area is near the junction. Mirbagheri et al. (2004) studied on the melt flow and effect of mould roughness of sand mould. Lee and Lee (2005) studied on the thermomechanical behaviour of sand casting using FEA. Kulkarni and Radhakrishna (2007) studied on the solidification time of a cylinder in sand mould in FEA technique using ANSYS FEA package. Kermanpur et al. (2008) studied on the melt flow and solidification in the multi-cavity mould for gray cast iron. Hsu et al. (2009) investigated on the multiple-gate runner system for gravity casting in sand mould in computational method. Fras et al. (2005) studied on the transition from gray to white during solidification for both mathematically and experimentally. They concluded that solidification rate depends on the modulus of the casting and the heat flow through the mould which was indicated the moulding materials.

Most of the researchers used aluminium alloy and green sand mould for their experimental investigation. However, the work on heat flow for the gray cast iron (GCI) casting through resin bonded sand mould is very limited in the literature. Therefore in the present study, an attempt has been made to simulate the heat flow condition that is how the heat flows through the resin bonded sand mould using FEA tools and to study the effect of heat flow on the microstructure and hardness of the GCI cast product. Finally, a correlation was obtained between simulation and experimental test results.

2. EXPERIMENTAL

The whole work divides into two parts. Firstly, the simulation of heat flow from liquid GCI metal to the sand mould was performed and secondly, the gray cast iron was cast to experimentally verify the model.

2.1 Simulation of Heat Flow

The heat conduction equation used in this research work to simulate the heat flow is,

$$\frac{\partial Q}{\partial t} = \frac{k}{C_P \rho}\left(\frac{\partial^2 Q}{\partial x^2} + \frac{\partial^2 Q}{\partial y^2}\right) \tag{1}$$

where, $\frac{\partial Q}{\partial t}$ is the rate of change of temperature at a point over time, k / $C_p\rho$ is the thermal diffusivity, k is material-specific quantity depending on the thermal conductivity, ρ is the mass density, and , cp is the specific heat capacity.

The Fourier's law of conduction also enclosed for the heat flow of the resin bonded sand mould and can be as expressed,

$$q = -kA\frac{dT}{dx} \tag{2}$$

where, A is the cross-sectional area, k is materials thermal conductivity, dT/dx is the temperature difference along the path.

The Newton’s law of cooling can be employed for the cooling rate of the liquid and the sand mould can be expressed as

$$\frac{dT}{dt} = -k(T - T_a) \tag{3}$$

where, T and Ta representing the temperatures of melt and mould, respectively.

The sand mould is not a completely compacted solid and there are a lot of pores which are filled with air and this air is considered as fluid (Sulaiman and Hamouda, 2004). The heat transfer from a solid surface to a fluid can be written as follows:

$$Q = \alpha A(T - T_a) \tag{4}$$

The total heat energy, Q in the liquid metal can be shown using the following equation:

$$Q = V\rho L \tag{5}$$

Where, V is the volume of the materials, ρ is the density of the liquid and L is the latent heat of the materials.

Finally, the heat flow was simulated using JL Analyzer, Auto FEA software for every 120 seconds. It was assumed that no heat losses occurred before filling the mould. The chemical composition of the gray cast iron and the thermal properties of materials (both GCI and resin bonded sand mould) are shown in Table 1 and Table 2 respectively.

Table 1: Chemical composition of the cast alloy

Chemical chemical elements (wt%)	Gray iron composition
C	2.870
Si	2.930
Al	0.150
Mn	0.350
P	0.040
S	0.020
Cr	0.064
Cu	0.244
Mg	0.002
Fe	Bal.

Table 2: Thermal properties of the materials

Properties	Resin bonded sand mould	Gray cast iron
Thermal conductivity, W m^{-1}. K	0.981	32.30
Density, g cm^{-3}	1.770	7.10
Specific heat, J Kg^{-1}. K	735.000	0.42
Latent heat of graphite, J cm^{-3}	-	2028.80
Latent heat of austenite, J cm^{-3}	-	1904.40
Liquidus temperature °C	-	1195.00
Solidus temperature °C	-	1123.00

Fig. 1 shows the 2D drawing of the pattern where mesh was generated using JL Analyzer FEA software. The mesh length was 5 mm and the materials properties were defined in the software. The mesh was loaded in the experimental condition that is the boundary conditions and then the initial conditions are applied. By running the analysis software, the heat flow through the mould was simulated.

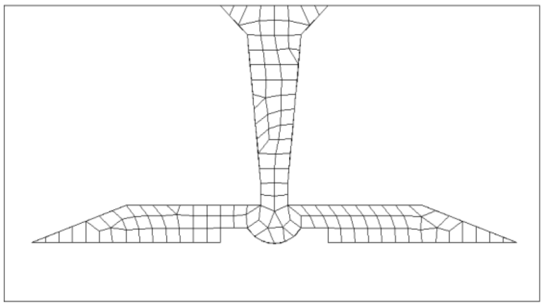

Figure 1 Pattern loaded in FEA software for analysis of sand mould

2.2 Moulding and Casting

For this study, synthetic silica sand, cold set asphalt resin and alpha cure hardener were used as moulding materials. To make the mould, silica sand was mixed with 2% resin for 5 minutes. Then, 1% cold set hardener was used and continued the mixing for 1 minute. Using this freshly prepared sand mixture, the mould was prepared using wooden pattern.

To melt the raw material, medium frequency induction furnace was used. Firstly, pig iron and mild steel were melted together and heated up to about 1350^{O}C. Then, fluxing material was added into the melt and stirred the melt thoroughly. Then, the slag was removed and ferrosilicon was added into the melt. Again, the fluxing material was added and slag was removed by keeping the melt in the furnace. When the melt was ready, the liquid metal was poured into the mould at about 1300^{O}C. After casting the condition of the mould was observed in terms of burning off of sand and heat affected area. For metallographic study, the sample was prepared by standard technique used in ASM metal handbook. Hardness values (HRB) of the cast materials were measured from 10 mm thickness to 2 mm thickness area using Rockwell hardness tester Model 660RLD/T.

3. RESULTS AND DISCUSSION

3.1 Heat Flow through the Sand Mould

The predicted heat flow condition through the sand mould with time is shown in Fig 2. It shows that the heat affected area increases increasing with time from 0 to 360 seconds and most of the heat energy is concentrated near the sprue where the thickness of the casting is 10 mm. When the casting thickness changes from 10 mm to 2 mm, the intensity of the heat decreases and solidification rate increases from 8.79 0C/S to 21.36 0C. This phenomenon can be explained using Fourier's law of heat conduction (equation 2) which states that the rate of heat flow through solid material is directly proportional to the cross sectional area and the temperature difference along the path of heat flow.

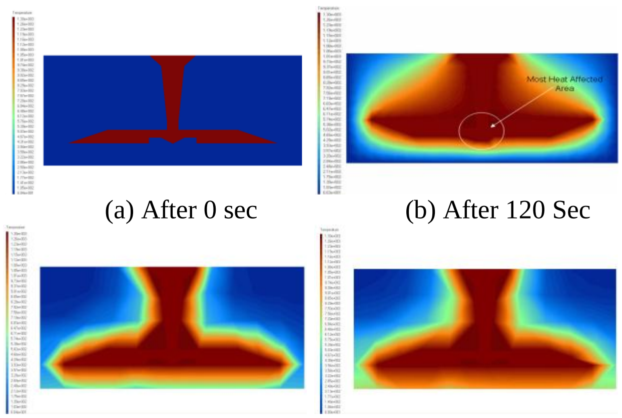

(a) After 0 sec (b) After 120 Sec

(c) After 240 sec (d) After 360 sec

Figure 2 Simulation of temperature distribution on the sand mould using FEA software.

The explanation for the cooling rate of the liquid metal in the sand mould casting can be interpreted with Newton's law of cooling (equation 3) which states that the rate of change of the temperature of an object is proportional to the difference between its own temperature and the ambient temperature.

The present findings of the cooling rate well agreed the previous law; hence, cooling rate increases with decreases the thickness. So, if the casting thickness is low, the total heat energy at that point will be low and will dissipate quickly. However for higher thickness, it will be just reverse.

3.2 Effect of Temperature Distribution on Sand

Fig. 3 shows actual temperature distribution on cold set resin bonded sand mould before and after casting. It can be seen that most heat most of the heat concentrated nearby the sprue area which is known as heat affected area (HAA) where the sand burn off and changes from reddish to black in colour. It can be attributed to the fact that higher flow of heat at the junctions of the runners and higher thickness of the mould cavity are responsible for intense heat nearby the sprue area. However, when the thickness of the mould decreases the HAA also decreases and this phenomenon can be seen in Fig. 2 the simulation of temperature distribution of the mould.

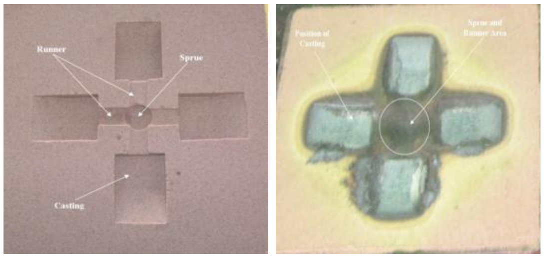

(a) (b)

Figure 3 Actual temperature distribution on cold set resin bonded sand mould, (a) before casting, (b) after casting

3.3 Microstructure

The microstructure was observed under optical microscope and is shown in Fig 4. It indicates that the 10 mm to 2 mm thickness areas show different microstructures due to different solidification rate (hence different heat dissipation rates) as already described in Fig 2. However, Fig 4 shows that there are three distinguished structural differences available in the cast product. Firstly, the gray type microstructure for 10 mm thickness which consists of graphite flakes in pearlite; secondly, mottle type for 7-4 mm thickness which consists of mixture of gray and white cast iron and last 3-2 mm thickness which is completely white cast iron.

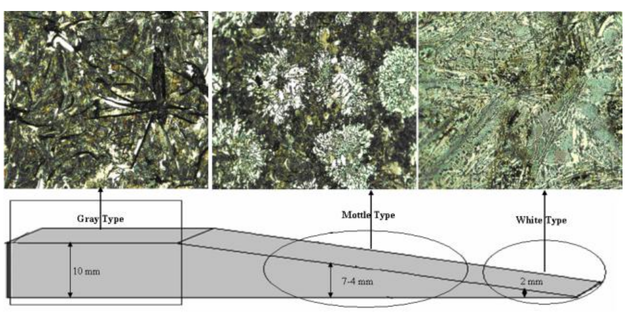

Figure 4 Microstructure of cast iron in various thicknesses; gray type (10 mm), mottle type (4-7 mm) and white type (2 mm)

These different microstructural phases at various thicknesses were due to the solidification rate difference of the melt during heat flow. The graphite flake (GCI) is an eutectic cell which is formed during slow cooling before the eutectoid isothermal temperature starts [Elliott, 1988]. When the heat energy was higher, the heat flows through the sand mould was lower which reduces the solidification rate of the cast iron and yield eutectic graphite cell. Again, in the lower thickness area, the absorption of heat energy in the sand mould was higher which increases the solidification rate of the melt. Therefore, there was not enough time to form eutectic graphite cell instead the austenite changes to cementite and pearlite phases.

It is believed incase of unalloyed castings that if the solidification rate is increased and crossed the critical value, it suppresses the graphitization process and promotes the formation of carbide which increased the formation of cementite or white cast iron phases [Giacchi et al., 2007]. Therefore, for the lower thickness of the cast product, white cast iron phase was formed instead of gray cast iron. Finally, it can be concluded that in this investigation, three distinct microstructures phases are formed such as gray, mottle and white due to three different cooling or solidification rate.

3.4 Hardness

Fig. 5 shows the hardness values of the cast materials at different thickness which is governed by the heat flow through the sand mould. It is clear that with decreasing the thickness, the hardness value increases and hardness value obtained here 78.71 HRB for 10 mm thickness whereas 95.10 HRB for 2 mm thickness. This is due to the fact that at 10 mm thickness area shows gray iron phase whereas 2 mm thickness shows white cast iron phase which are responsible for the different hardness values of the final casting. In this section, the liquid metal solidifies rapidly; as a result the carbon cannot get enough time to come out from the austenite solution. Again, in thick area (10 mm) the solidification rate is comparatively lower and the graphite easily forms and separates out from the liquid metal and hence, lower value of hardness [Haque and Young, 1995].

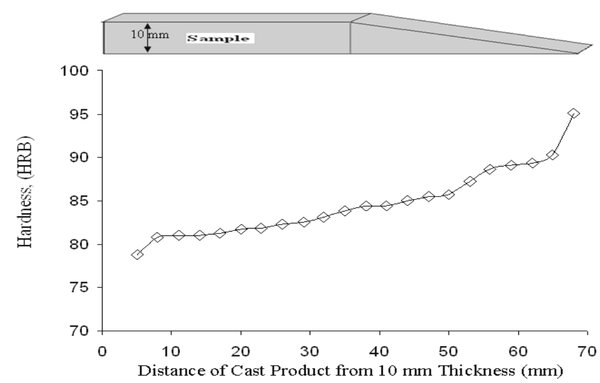

Figure 5 Hardness of the casting from 10 mm to 2 mm thickness in 70 mm length, indentation was made after 2 mm distance

The volume of the 10 mm thickness area is higher than that of 2 mm thickness area. According to the Equation 4, density and latent heat of the materials are constant, so the total heat energy in the mould is proportional to the volume of the liquid metal which is higher in the 10 mm thickness area and sand in this area becomes more heated than 2 mm thickness area. At the same time, the heat extraction rate is higher in the 2 mm thickness area than the 10 mm thickness area. As a result, the hardness values and microstructures of cast iron are different from one end to the other end of the casting, which has been demonstrated in Fig 5.

3.5 Significance and Limitation

The main assumption of the model is no heat loss before completely filling the mould but in practice as soon as the liquid metal enters into the mould cavity, it starts to fall its temperature and changes the microstructure. The simulation shows that the most heated area is near the sprue where the thickness is 10 mm. However, it is not only the thickness but also the junction of the design. Similar observation was reported by Sulaiman and Hamouda, 2004. Using this model, it is successfully possible to predict the heat-flow through the sand mould and the related microstructures of cast product.

4. CONCLUSIONS

From the present study, the following conclusions can be drawn:

a. The simulation of heat flow (HF) condition using FEA software on the sand mould was found that HF decreases with decreasing of casting thickness from 10 mm to 2 mm. However, solidification rate increases for the same condition.
b. Different microstructure was obtained for different HF for the same chemical composition of the material due to different solidification rate. The three distinct microstructural phases were gray, mottle and white.
c. The lower hardness values were obtained at higher thickness area whereas higher hardness values were attained at lower thickness area.
d. Finally, it can be summarized that by controlling the heat following direction through the sand mould materials structure as well as properties can be controlled.

ACKNOWLEDGMENT

Authors are thankful to the Faculty of Engineering, International Islamic University Malaysia for providing lab facilities and Fundamental Research Grand Scheme (FRGS 01-06-01) for finincial support.

REFERENCES

Al-Asady, N. A., Abdullah, S., Ariffin, A. K., Beden, S. M., and Rahman, M. M., 2009. FEA Based Durability Using Strain-Life Models For Different Medium Carbon Steel As Fabrication Materials For An Automotive Component, International Journal of Mechanical and Materials Engineering, 4 (2), 141-146.

ASM Metal Handbook, 1997. Metallography and Microstructure, volume 9, ASM International, Materials Park, Ohio.

Chao, L. S. and Du, W. C., 1999. Macro-micro modeling of solidification, Procedings of Natural Scientific Conference, ROC (A), World Scientific Publisher, China, 23 (5), 622-629.

Elliott, R. 1988. Cast Iron Technology, 1st Ed. Butterworth & Co., UK.

Fras, E., Gorny, M. and Lopez, H. F., 2005. The Transition from Gray to white cast iron during solidification: part I. Theoretical background, Metallurgical and Materials Transactions A, 36, 3075-82.

Fras, E., Gorny, M. and Lopez, H. F., 2005. The Transition from gray to white cast iron during solidification: part II. Experimental verification, Metallurgical and Materials Transactions A, 36, 3083-92.

Ghaderi, A. R., Ahmadabadi, M. N., and Ghasemi, H. M., 2003. Effect of graphite morphologies on the tribological behaviour of austempered cast iron, Wear, 255, 410–416.

Hsu, F. Y., M. R. Jolly and J. Campbell, 2009. A multiple-gate runner system for gravity casting, Journal of Materials Processing Technology, 209, 5736-5750.

Kermanpur, A., Mahmoudi, S. and Hajipour, A. 2008. Numerical simulation of metal flow and solidification in the multi-cavity casting moulds of automotive components, Journal of Materials Processing Technology, Volume 206, pp. 62–68.

Kulkarni, S. N. and Radhakrishna, K., 2007. Prediction of solidification time of cylindrical hollow casting cast in CO2-Sand moulds by using FEA Technique, International Journal of Materials Science, 2(2), 137-152.

Lee, S. M. and Lee, W. J., 2005. Finite-Element analysis on thermomechanical behaviour of a marine propeller casting in the sand casting process, Journal of Materials Engineering and Performance, 14 (3), 388-394.

Mirbagheri, S. M. H., Dadashzadeh, M., Serajzadeh, S., Taheri, A. K., and Davami, P., 2004. Modeling the effect of mould wall roughness on the melt flow simulation in casting process, Applied Mathematical Modelling, 28, 933–956.

Pequet, C., Gremaud, M. and Rappaz, M., 2002. Modeling of microprosity, macroporosity and pipe-shrinkage formation during the solidification of alloys using a mushy-zone refinement method: Applications to Aluminium alloys, Metallurgical and Materials Transaction A, 33, 2095-2106.

Seetharamu, K. N., Paragasam, R., Quadir, G. A., Zainal, Z. A., Prasad, B. S. A., and Sundararajan, T., 2001. Finite element modeling of solidification

phenomena, Indian Academy of Sciences, 26 (1&2), 102-120.
Sulaiman, S. and Hamouda, A. M. S., 2004. Modeling of the thermal history of the sand casting process, Journal of Materials Processing Technology, 150 (3), 242-254.
Haque M. M. and Young, J. M., 1995. Production of spheroidal graphite aluminium cast iron and the factors affecting it, Journal of Materials Processing Technology, 55 (3), 186-192.